Stochastic Fatigue Analysis of Jacket Type Offshore Structures

Sigurdsson, Gudfinnur

Publication date:
1988

Document Version
Publisher's PDF, also known as Version of record

INSTITUTTET FOR BYGNINGSTEKNIK

INSTITUTE OF BUILDING TECHNOLOGY AND STRUCTURAL ENGINEERING

AALBORG UNIVERSITETSCENTER · AUC · AALBORG · DANMARK

STRUCTURAL RELIABILITY THEORY

PAPER NO. 50

Presented at the 2nd IFIP WG 7.5 Working Conference on »Reliability and Optimization of Structural Systems», London, September 26 - 28, 1988

G. SIGURDSSON

STOCHASTIC FATIGUE ANALYSIS OF JACKET TYPE OFFSHORE STRUCTURES

SEPTEMBER 1988

ISSN 0902-7513 R8828

The STRUCTURAL RELIABILITY THEORY papers are issued for early dissemination of research results from the Structural Reliability Group at the Institute of Building Technology and Structural Engineering, University of Aalborg. These papers are generally submitted to scientific meerings, conferences or journals and should therefore not be widely distributed. Whenever possible, reference should be given to the final publications (proceedings, journals, etc.) and not to the Structural Reliability Theory papers.

INSTITUTTET FOR BYGNINGSTEKNIK
INSTITUTE OF BUILDING TECHNOLOGY AND STRUCTURAL ENGINEERING
AALBORG UNIVERSITETSCENTER · AUC · AALBORG · DANMARK

STRUCTURAL RELIABILITY THEORY
PAPER NO. 50

Presented at the 2nd IFIP WG 7.5 Working Conference on »Reliability and Optimization of Structural Systems», London, September 26 - 28, 1988

G. SIGURDSSON

STOCHASTIC FATIGUE ANALYSIS OF JACKET TYPE OFFSHORE STRUCTURES

SEPTEMBER 1988 ISSN 0902-7513 R8828

PROBABILISTIC FATIGUE ANALYSIS OF OFFSHORE STRUCTURES

G. Sigurdsson

Institute of Building Technology and Structural Engineering
University of Aalborg, Denmark

1. INTRODUCTION

Offshore structures of all types are generally subjected to cyclic loading from wind, current earthquakes and waves acting simultaneously, which cause time-varying stresses in the structure. The environmental quantities are of a random nature and are more or less correlated to each other through the generating and driving mechanism. Waves and earthquakes are generally considered to be the most important sources of the structural excitations. However, earthquake loads are only taken into account in the analysis of offshore structures close to or in tectonic offshore fields. For fixed offshore structures in deep water environments wind loads represent a contribution of about 5 % to the environmental loading [1]. Current loads are mostly considered to be unimportant in the dynamic analysis of offshore structures, because their frequencies are not sufficient to excite the structures. The reliability calculation of offshore structures is a difficult task due to the random nature of the loading, and also due to insufficient information of structural failure under these conditions. A stochastic assessment of the reliability analysis of structures is therefore inevitable. Dynamic loads, such as wave loads, produce stress fluctuations in the structural members and joints and are the primary cause of fatigue damages. A fatigue analysis of offshore structures can be described in general terms as a calculation procedure, starting from the waves and ending with a fatigue damage occurring in the material or in the joints. The links between the waves and the damage are formed by mathematical models for the wave forces, the structural behaviour and the material behaviour. I view of the stochastic and dynamic character of the waves it is an obvious choice to apply spectral fatigue analysis methods to the fatigue problem. In this paper, a stochastic reliability assessment for jacket type offshore structures subjected to wave loads in deep water environments is outlined. In the reliability assessment, structural and loading uncertainties are taken into account by means of some stochastic variables. To estimate statistical measures of structural stress variations the modal spectral analysis method is applied.

The analysis is divided into four steps:

I Description of the sea state
   a) short-term model
   b) long-term model

II Description of the wave loading

III Structural analysis

IV Fatigue analysis

2. DESCRIPTION OF THE SEA STATE

Short-term model:
The observed sea elevation at the fixed location $\overline{r}$ at the time t, $\eta(\overline{r},t)$, can be considered as a realization of non-stationary stochastic process, whose characteristic parameters vary slowly with time. Further, we assumed that for short-term periods (a few hours) the sea surface $\eta(\overline{r},t)$ can be considered as a realization of a stationary stochastic process. This process is assumed to be a zero-mean ergodic Gaussian process. The cross-spectral density of the sea surface at the points n and m (with spatial coordinates (x_n, y_n) and (x_m, x_m), respectively) can be written as:

$$S_{\eta_n\eta_m}(\omega) = S_{\eta\eta}(\omega) \int_\theta \psi(\theta)\ exp(-\epsilon\kappa(\omega)(\Delta x cos\theta + \Delta y sin\theta))d\theta \tag{1}$$

where $\epsilon = \sqrt{-1}$, $\Delta x = (x_n - x_m)$, $\Delta y = (y_n - y_m)$ and κ is the wave number, defined as:

$$\omega^2 = \kappa\ g\ tanh(\kappa d) \quad ; \quad \omega \geq 0.0 \quad , \quad \kappa \geq 0.0 \tag{2}$$

Serveral analytical expressions have been suggested for the spreading function $\psi(\theta)$. Generally, a cosine function is used:

$$\psi(\theta) = \begin{cases} K\ cos^{2n}(\theta - \overline{\theta}) & -\frac{\pi}{2} \leq (\theta - \overline{\theta}) \leq \frac{\pi}{2} \\ 0 & \text{elsewhere} \end{cases} \tag{3}$$

Where $\overline{\theta}$ denotes the average direction of wave propagation and K is a normalization factor defined so that the spreading function between $-\frac{\pi}{2}$ and $\frac{\pi}{2}$ is equal to one:

$$K = \frac{1}{\sqrt{\pi}} \frac{\Gamma(n+1)}{\Gamma(n+\frac{1}{2})} \tag{4}$$

where Γ is the Gamma function and n is a parameter defining the width of the distribution. For the limiting case $n = 0$ eq.(3) approaches the Dirac delta function corresponding to long-crested waves.

Here, the JONSWAP spectrum is adopted as a reasonable model of the sea surface, $S_{\eta\eta}$. This spectrum reads [6]:

$$S_{\eta\eta}(\omega) = \alpha\, g^2 \omega^{-5} exp\left(-\frac{5}{4}\left(\frac{\omega}{\omega_p}\right)^{-4}\right)\gamma^{exp\left(-\frac{1}{2}\left(\left(\frac{\omega}{\omega_p}-1\right)/\sigma\right)^2\right)} \tag{5}$$

where

- ω is the frequency (rad/sec)
- α is the equlibrium range parameter
- g is the acceleration of gravity
- ω_p is the spectral peak $(= 2\pi/T_p\ )$
- γ is the spectral peak parameter
- σ is the spectral peak width parameter (here taken as 0.08)

Long-term model:
As mentioned earlier, it is assumed that the sea surface elevation at a fixed location for stort-term periods can be accurately modelled by a zero-mean ergodic Gaussian process. This process is completely characterized by the frequency spectrum $S_{\eta\eta}(\omega)$ which, for a given average direction of wave propagation $\overline{\theta}$, can be described by two parameters, namely by the significant wave heigh

H_s and the spectral peak periods T_p. The long-term probability distribution of the sea state is then given as a joint distribution of $\overline{\theta}, H_s$ and T_p , $p_{H_s T_p \overline{\theta}}(h,t,\theta)$. It is not possible to establish this distribution theoretically. The distribution has to be estimated from wave observations in the ocean area concerned or derived applying hidcasting models, i.e. the chosen analytical model has to be fitted in the best possible way to the data.
In most wave observations up till now no information of the mean direction of propagagion $\overline{\theta}$ has been included. If it is assumed that the joint distribution of H_s and T_p is independent of $\overline{\theta}$, the joint distribution $p_{H_s T_p \overline{\theta}}(h,t,\theta)$ can be written as:

$$p_{H_s T_p \overline{\theta}}(h,t,\theta) = p_{H_s T_p}(h,t)\; p_{\overline{\theta}}(\theta) \tag{6}$$

For our purpose the probability density function $p_{H_s T_p}(h,t)$ is conveniently written as:

$$p_{H_s T_p}(h,t) = p_{T_p|H_s}(t|h)\, p_{H_s}(h) \tag{7}$$

where $p_{H_s}(h)$ is the marginal probability density function for H_s and $p_{T_p|H_s}(t|h)$ is the conditional probability density function for T_p given H_s. $p_{H_s}(h)$ and $p_{T_p|H_s}(t|h)$ are fitted to the observations separately. The numerical values for $p_{H_s T_p}(h,t)$ are obtained by means of eq.(7). Here $p_{H_s}(h)$ is modelled by log-normal distribution for $H_s \leq v$ and by Weibull distribution for $H_s < v$, i.e.

$$p_{H_s} = \begin{cases} \frac{1}{\sqrt{2\pi}\sigma_{H_s} h}\; exp\left(\frac{-(ln\, h - \mu_{H_s})^2}{2\sigma^2_{H_s}}\right) & h \leq v \\ \frac{\xi}{\rho}\left(\frac{h}{\rho}\right)^{\xi-1}\; exp\left(-\frac{h}{\rho}\right)^{\xi} & \rho > 0\;, \xi > 0\;, h > v \end{cases} \tag{8}$$

where μ_{H_s} and $\sigma^2_{H_s}$ are the mean and variance of the variable $ln\,(H_s)$, respectively, and where continuity is required for $p_{H_s}(h)$ and $P_{H_s}(h)$ at $h{=}v$. The conditional distribution of T_p given H_s is approximated by the log-normal distribution, i.e.

$$p_{T_p|H_s}(t|h) = \frac{1}{\sqrt{2\pi}\sigma_{T_p} t}\; exp\left(\frac{-(ln\, t - \mu_{T_p})^2}{2\sigma^2_{T_p}}\right) \tag{9}$$

where μ_{T_p} and $\sigma^2_{T_p}$ are the mean and variance of the variable $ln\,(T_p)$, respectively.
The marginal probability density function $p_{\overline{\theta}}(\theta)$ will divide the circle into a certain number of sectors and associate each sector with a point probability $p_{\overline{\theta}}(\theta_k), k = 1, ..., n$ where θ_k is the midpoint of sector no. k and n is the number of sectors.

3. DESCRIPTION OF THE WAVE LOADING

In chapter 2 the statistical nature of the waves was dealt with. Now the consequential loading on a structural element is considered. It is well known that the force on a vertically placed circular cylinder subjected to wave action consists of a drag as well as an inertia component. It is assumed that Morison's equation can be applied to a cyndrical member oriented in a random manner. The total wave force per unit length of cylinder of the diameter D at the position $\overline{r}_0 = (x_0, y_0, z_0)$ at the time t is:

$$\overline{f}_n(\overline{r}_0, t) = \begin{bmatrix} f_{nx}(\overline{r}_0, t) \\ f_{ny}(\overline{r}_0, t) \\ f_{nz}(\overline{r}_0, t) \end{bmatrix} = \overline{f}_{nD} + \overline{f}_{nI} \tag{10}$$

where

$\overline{f}_{nD} = K_D \, |\dot{\overline{u}}_n(\overline{r}_0,t)| \, \dot{\overline{u}}_n(\overline{r}_0,t)$

$\overline{f}_{nI} = K_I \, \ddot{\overline{u}}_n(\overline{r}_0,t)$

$K_D = 1/2\, C_D \, \rho D$

$K_I = 1/4\, C_M \, \pi \, \rho \, D^2$

$\dot{\overline{u}}(\overline{r}_0,t)$ is the horizontal water particle velocity at the position $\overline{r}_0$ at the time t.

$\ddot{\overline{u}}(\overline{r}_0,t)$ is the horizontal water particle acceleration at the position $\overline{r}_0$ at the time t.

x, y, z is the global coordinate system.

C_D is the drag coefficient.

C_M is the inertia coefficient.

ρ is the density of water.

and where the subscript n refers to the normal direction of the cylinder.
The non-linear drag term $\overline{f}_{nD}$ in eq.(10) makes the computations for correlations and spectral densities extremely difficult and intractable, and therefore, a recourse to linearization of the drag term in eq.(10) is made. The "minimum square error linearization method" [9] is used here. The linearized version of the drag term $\overline{f}_{nD}$ becomes :

$$\overline{f}_{DL} = K_D \, \overline{\overline{L}} \, \dot{\overline{u}}_n(\overline{r}_0,t) = K_D \begin{bmatrix} l_{11} & l_{12} & l_{13} \\ l_{21} & l_{22} & l_{23} \\ l_{31} & l_{32} & l_{33} \end{bmatrix} \begin{bmatrix} \dot{u}_{nx} \\ \dot{u}_{ny} \\ \dot{u}_{nz} \end{bmatrix} \tag{11}$$

where $\overline{\overline{L}}$ is the linearization coefficient matrix which is given in appendix A.
Eq.(11) can now be written as:

$$\overline{f}_n(\overline{r}_0,t) = \begin{bmatrix} f_{nx}(\overline{r}_0,t) \\ f_{ny}(\overline{r}_0,t) \\ f_{nz}(\overline{r}_0,t) \end{bmatrix} = K_D \, \overline{\overline{L}} \, \dot{\overline{u}}_n(\overline{r}_0,t) + K_I \ddot{\overline{u}}_n(\overline{r}_0,t) \tag{12}$$

The normal vectors $\dot{\overline{u}}_n$ and $\ddot{\overline{u}}_n$ in eq.(12) can be expressed in terms of a unit vector $\overline{c} = (c_x, c_y, c_z)$ along the cylinder axis as follows (see Appendix A):

$$\dot{\overline{u}}_n = \overline{c} \times (\overline{\dot{u}^T} \times \overline{c}) = \overline{\overline{C}} \, \dot{\overline{u}}$$

$$\ddot{\overline{u}}_n = \overline{c} \times (\overline{\ddot{u}^T} \times \overline{c}) = \overline{\overline{C}} \, \ddot{\overline{u}} \tag{13}$$

where

$$\overline{\overline{C}} = \begin{bmatrix} (1-c_x^2) & -c_x c_y & -c_x c_z \\ & (1-c_y^2) & -c_y c_z \\ \text{sym.} & & (1-c_z^2) \end{bmatrix} = \left[\{\overline{C}\}_x \; \{\overline{C}\}_y \; \{\overline{C}\}_z \right]$$

$$\dot{\overline{u}} = \begin{bmatrix} \dot{u}_x \\ \dot{u}_y \\ \dot{u}_z \end{bmatrix} \quad ; \quad \ddot{\overline{u}} = \begin{bmatrix} \ddot{u}_x \\ \ddot{u}_y \\ \ddot{u}_z \end{bmatrix}$$

Now eq.(12) can be rewritten as:

$$\overline{f}_n(\overline{r}_0,t) = \begin{bmatrix} f_{nx}(\overline{r}_0,t) \\ f_{ny}(\overline{r}_0,t) \\ f_{nz}(\overline{r}_0,t) \end{bmatrix} = K_D \, \overline{\overline{L}} \, \overline{\overline{C}} \, \dot{\overline{u}}(\overline{r}_0,t) + K_I \, \overline{\overline{C}} \, \ddot{\overline{u}}(\overline{r}_0,t) \tag{14}$$

Two points in the wave field are considered, i.e. point l with the coordinates $\overline{r}_l = (x_l, y_l, z_l)$ and point m with the coordinates $\overline{r}_m = (x_m, y_m, z_m)$. l denotes a circular cylindrical element L with the diameter D_L and the unit vector $\overline{c}_L = (c_{x_L}, c_{y_L}, c_{z_L})$ along the cylinder axis and point m denotes a circular cylindrical element M with the diameter D_M and the unit vector $\overline{c}_M = (c_{x_M}, c_{y_M}, c_{z_M})$ along the cylinder axis. The cross-covariance function for the various combinations of wave force components at l and m can now be expressed as a function of the covariance functions of $\overline{u}$ and $\overline{\dot{u}}$. The cross-spectral densities between various components can be found by deriving the Fourier transforms of the corresponding cross-covarince functions. The cross-spectral density between the forces f_{nil} and f_{nim} becomes (subscripts nil and njm $(i,j = x,y,z)$ denote the force perpendicular to the elements in the directions i and j at the points l and m):

$$\begin{aligned} S_{f_{nil}f_{njm}}(\omega) &= K_{D_L}\, K_{D_M}[(\{\overline{B}_l\}_i\ \{\overline{B}_m\}_j)]\ [S_{\dot{u}_l\dot{u}_m}] \\ &+ K_{D_L}\, K_{I_M}[(\{\overline{B}_l\}_i\ \{\overline{C}_M\}_j)]\ [S_{\dot{u}_l\ddot{u}_m}] \\ &+ K_{I_L}\, K_{D_M}[(\{\overline{C}_L\}_i\ \{\overline{B}_m\}_j)]\ [S_{\ddot{u}_l\dot{u}_m}] \\ &+ K_{I_L}\, K_{I_M}[(\{\overline{C}_L\}_i\ \{\overline{C}_M\}_j)]\ [S_{\ddot{u}_l\ddot{u}_m}] \end{aligned} \tag{15}$$

where

$$[\{\overline{B}_l\}_x\ \{\overline{B}_l\}_y\ \{\overline{B}_l\}_z] = \overline{\overline{L}}_l\ \overline{\overline{C}}_L$$

$$[\{\overline{B}_m\}_x\ \{\overline{B}_m\}_y\ \{\overline{B}_m\}_z] = \overline{\overline{L}}_m\ \overline{\overline{C}}_M$$

$$\overline{\overline{C}}_L = [\{\overline{C}_L\}_x\ \{\overline{C}_L\}_y\ \{\overline{C}_L\}_z] = \begin{bmatrix} (1-c_{x_L}^2) & -c_{x_L}c_{y_L} & -c_{x_L}c_{z_L} \\ & (1-c_{y_L}^2) & -c_{y_L}c_{z_L} \\ \text{sym.} & & (1-c_{z_L}^2) \end{bmatrix}$$

$$\overline{\overline{C}}_M = [\{\overline{C}_M\}_x\ \{\overline{C}_M\}_y\ \{\overline{C}_M\}_z] = \begin{bmatrix} (1-c_{x_M}^2) & -c_{x_M}c_{y_M} & -c_{x_M}c_{z_M} \\ & (1-c_{y_M}^2) & -c_{y_M}c_{z_M} \\ \text{sym.} & & (1-c_{z_M}^2) \end{bmatrix}$$

$\overline{\overline{L}}_l$ and $\overline{\overline{L}}_m$ are the linearization coefficient matrices for point l and point m, respectively.

$$[S_{\dot{u}_l\dot{u}_m}] = \begin{bmatrix} S_{\dot{u}_{x_l}\dot{u}_{x_m}}(\omega) & S_{\dot{u}_{x_l}\dot{u}_{y_m}}(\omega) & S_{\dot{u}_{x_l}\dot{u}_{z_m}}(\omega) \\ S_{\dot{u}_{y_l}\dot{u}_{x_m}}(\omega) & S_{\dot{u}_{y_l}\dot{u}_{y_m}}(\omega) & S_{\dot{u}_{y_l}\dot{u}_{z_m}}(\omega) \\ S_{\dot{u}_{z_l}\dot{u}_{x_m}}(\omega) & S_{\dot{u}_{z_l}\dot{u}_{y_m}}(\omega) & S_{\dot{u}_{z_l}\dot{u}_{z_m}}(\omega) \end{bmatrix}$$

$$[S_{\dot{u}_l\ddot{u}_m}] = \begin{bmatrix} S_{\dot{u}_{x_l}\ddot{u}_{x_m}}(\omega) & S_{\dot{u}_{x_l}\ddot{u}_{y_m}}(\omega) & S_{\dot{u}_{x_l}\ddot{u}_{z_m}}(\omega) \\ S_{\dot{u}_{y_l}\ddot{u}_{x_m}}(\omega) & S_{\dot{u}_{y_l}\ddot{u}_{y_m}}(\omega) & S_{\dot{u}_{y_l}\ddot{u}_{z_m}}(\omega) \\ S_{\dot{u}_{z_l}\ddot{u}_{x_m}}(\omega) & S_{\dot{u}_{z_l}\ddot{u}_{y_m}}(\omega) & S_{\dot{u}_{z_l}\ddot{u}_{z_m}}(\omega) \end{bmatrix}$$

$$[S_{\ddot{u}_l\dot{u}_m}] = \begin{bmatrix} S_{\ddot{u}_{x_l}\dot{u}_{x_m}}(\omega) & S_{\ddot{u}_{x_l}\dot{u}_{y_m}}(\omega) & S_{\ddot{u}_{x_l}\dot{u}_{z_m}}(\omega) \\ S_{\ddot{u}_{y_l}\dot{u}_{x_m}}(\omega) & S_{\ddot{u}_{y_l}\dot{u}_{y_m}}(\omega) & S_{\ddot{u}_{y_l}\dot{u}_{z_m}}(\omega) \\ S_{\ddot{u}_{z_l}\dot{u}_{x_m}}(\omega) & S_{\ddot{u}_{z_l}\dot{u}_{y_m}}(\omega) & S_{\ddot{u}_{z_l}\dot{u}_{z_m}}(\omega) \end{bmatrix}$$

$$[S_{\ddot{u}_l\ddot{u}_m}] = \begin{bmatrix} S_{\ddot{u}_{x_l}\ddot{u}_{x_m}}(\omega) & S_{\ddot{u}_{x_l}\ddot{u}_{y_m}}(\omega) & S_{\ddot{u}_{x_l}\ddot{u}_{z_m}}(\omega) \\ S_{\ddot{u}_{y_l}\ddot{u}_{x_m}}(\omega) & S_{\ddot{u}_{y_l}\ddot{u}_{y_m}}(\omega) & S_{\ddot{u}_{y_l}\ddot{u}_{z_m}}(\omega) \\ S_{\ddot{u}_{z_l}\ddot{u}_{x_m}}(\omega) & S_{\ddot{u}_{z_l}\ddot{u}_{y_m}}(\omega) & S_{\ddot{u}_{z_l}\ddot{u}_{z_m}}(\omega) \end{bmatrix}$$

The brackets [...][...] in eq.(15), and later in eq.(18), are not matrix multiplications in the conventional sense, they are used here only to denote a row-to-column multiplication. After one row-to-column multiplication a sum is made and added to the sum of the second row-to-column multiplication and so on, so that the final result is only a single term. The cross-spectral densities of the water particle velocity $[S_{\dot{u}_l \dot{u}_m}]$ may be expressed in terms of the one-dimensional wave spectral density $S_{\eta\eta}(\omega)$ by using eq.(1) as, [2]:

$$[S_{\dot{u}_l \dot{u}_m}] = S_{\eta\eta}(\omega) \int_\theta \omega^2 \overline{\overline{\Lambda}}(\omega, z_l, z_m) \psi(\theta) exp(-\epsilon\kappa(\omega)(\Delta x \, cos\theta + \Delta y \, sin\theta)) d\theta \qquad (16)$$

where

$$\overline{\overline{\Lambda}}(\omega, z_l, z_m) = \overline{A}(\overline{\kappa}(\omega), z_l) \overline{A}^{*T}(\overline{\kappa}(\omega), z_m)$$

$$\overline{A}(\overline{\kappa}(\omega), z) = \frac{1}{sinh(\kappa(\omega)d)} \begin{bmatrix} cos\theta \; cosh(\kappa(\omega)z) \\ sin\theta \; cosh(\kappa(\omega)z) \\ \epsilon \; sinh(\kappa(\omega)z) \end{bmatrix}$$

$*$ denotes complex conjugated

ϵ $= \sqrt{-1}$

d is the water depth

Δx $= x_l - x_m$

Δy $= y_l - y_m$

$\kappa(\omega)$ is the wave number, defined in eq.(7)

$\psi(\theta)$ is the spreading function, defined in eq.(19)

The z-coordinates are measured from the bottom positive upwards.

The cross-spectral densities of water particle accelerations $[S_{\ddot{u}_l \ddot{u}_m}]$, acceleration and velocity $[S_{\ddot{u}_l \dot{u}_m}$ and velocity and acceleration $[S_{\dot{u}_l \ddot{u}_m}]$ can be obtained using the properties of the derived processes This gives:

$$[S_{\ddot{u}_l \ddot{u}_m}] = \omega^2 [S_{\dot{u}_l \dot{u}_m}] \qquad (17$$

$$[S_{\dot{u}_l \ddot{u}_m}] = -[S_{\ddot{u}_l \dot{u}_m}] = \epsilon\omega \, [S_{\dot{u}_l \dot{u}_m}]$$

Applying eq.(17), eq.(15) can be rewritten as:

$$S_{f_{nil} f_{njm}}(\omega) = [K_{D_L} \; K_{D_M}(\{\overline{B}_l\}_i \{\overline{B}_m\}_j) + \omega^2 K_{I_L} \; K_{I_M}(\{\overline{C}_L\}_i \{\overline{C}_M\}_j)$$

$$+ \epsilon\omega(K_{D_L} K_{I_M}(\{\overline{B}_l\}_i \; \{\overline{C}_M\}_j) - K_{I_L} K_{D_M}(\{\overline{C}_L\}_i \; \{\overline{B}_m\}_j))] \; [S_{\dot{u}_l \dot{u}_m}] \qquad (18$$

4. STRUCTURAL ANALYSIS

It is assumed that the structure can be modelled as a space frame of three-dimensional bear elements connected by nodal points, where each structural member in the structure has one o more elements. If the structural system is modelled by a linear system and by a finite number o degrees of freedom then the dynamic equations may written as:

$$\overline{\overline{M}} \, \ddot{\overline{x}} + \overline{\overline{C}} \, \dot{\overline{x}} + \overline{\overline{K}} \, \overline{x} = \overline{F} \qquad (19$$

where

$\overline{x}$ is the displacement vector

$\overline{\overline{M}}$ is the mass matrix

$\overline{\overline{C}}$ is the damping matrix

$\overline{\overline{K}}$ is the stiffness matrix

$\overline{F}$ is the load vector which varies with time

The matrix equation (19) represents a finite number of coupled differential equations. In this paper it is chosen to use a "modal analysis" to transform the coupled system into an uncoupled system. The uncoupled system becomes:

$$\ddot{q}_j + 2\zeta_j\omega_j\dot{q}_j + \omega_j^2 q_j = f_j \tag{20}$$

where q_j is the modal coordinates , ζ_j is the damping ratio and ω_j is the j^{th} natural frequency. The stresses $\overline{s}$ at internal points in the structure may be found as:

$$\overline{s} = \overline{\overline{T}}\,\overline{q} \tag{21}$$

where the components T_{ij} in the matrix $\overline{\overline{T}}$ indicate the stress at point i due to displacement in mode j, and $\overline{q}$ is the solution of eq.(20). The cross-spectral density of the stresses at points k and l may be written as (see eq.(21)):

$$S_{s_k s_l}(\omega) = \sum_{i=1}^{n}\sum_{j=1}^{n} T_{ki}T_{lj}S_{q_i q_j}(\omega) \tag{22a}$$

where

$$S_{q_i q_j}(\omega) = H^*_{q_i f_i}(\omega)H_{q_j f_j}(\omega)S_{f_i f_j}(\omega) \tag{22b}$$

$$H_{q_i f_i}(\omega) = \frac{1}{\omega_i^2 - \omega^2 + 2\epsilon\zeta_i\omega\omega_i} \tag{22c}$$

$$S_{f_i f_j}(\omega) = \sum_{r=1}^{m}\sum_{s=1}^{m} \phi_{ir}\phi_{js}S_{F_r F_s}(\omega) \tag{22d}$$

and where n is the number of mode shapes, $*$ denotes the complex conjugate, $\epsilon = \sqrt{-1}$, ϕ_{ir} is the (i,r) element in the mode shape matrix and m is the number of degrees of freedom.
The cross-spectral density of the load at the points r and s, $S_{F_r F_s}$, may be found as shown in chapter 3 (see eq.(18)).
For the fatigue analysis in chapter 5 the cross-spectral density of the stresses as a whole is not interesting. However, three characteristics, namely the area m_0, the second moment m_2 and the fourth moment m_4 of the auto-spectral density (i.e. $k = l$ in eq.(22a)) are of interest. The area of the auto-spectral density can be derived as:

$$m_0(s_k) = \sigma^2(s_k) = \int_0^\infty S_{s_k s_k}(\omega)d\omega \tag{23}$$

and the second and the fourth moment of the auto-spectral density as:

$$m_2(s_k) = \int_0^\infty \omega^2 S_{s_k s_k}(\omega) d\omega \tag{24}$$

$$m_4(s_k) = \int_0^\infty \omega^4 S_{s_k s_k}(\omega) d\omega \tag{25}$$

5. FATIGUE ANALYSIS

In chapter 4 it was shown how the spectral densities of the stresses in a given hot spot in the structure can be estimated. Here fatigue damage is defined as a result of cumulative damage because of stress fluctuations (the stress amplitude).

For a short-term period the sea state is assumed to be a zero-mean ergodic Gaussian process, see chapter 2. By using the linearized version of the Morison equation (see chapter 3), and by modelling the structural system linearly (see chapter 4) the stress response S becomes a zero-mean ergodic Gaussian process too.
A number of cycles counting algoritms have been proposed, see i.e. [20]. Two of the counting methods, namely the range count method (RC) and the rainflow count method (RFC) are generally recognized as the method which produces the best results, and they will be included here. Both methods give the same result for an ideal narrow-band stress history, but for wide-banded stress history the result can be very different.

In section 5.1 it will be shown how the probability of fatigue failure can be estimated by using Miner's rule and the so-called S-N approach.

5.1 Reliability Analysis

The relationship between the stress fluctuation and the damage can be found by using Miner's rule, witch states in essence that every stress cycle i results in the degree of damage D_i equal to

$$D_i = \frac{1}{N_i} \tag{26}$$

where N_i is the number of cycles to failure, if the same stress cycle is repeated over and over again. The most commonly used model to determine N_i is the so-called $S - N$ approach [14]:

$$N_i = \left(\frac{2S_i}{K}\right)^{-m} \tag{27}$$

where S_i is the stress amplitude and K and m are constants which can be determined by constant-amplitude test. To allow for the scatter in the number of cycles to fatigue and to allow for a model uncertainty by using Miner's rule, K and m are modelled as random variables. To allow for the uncertainty in the estimation of the stress amplitude a new random variable B will be introduced into eq.(27) as:

$$N_i = \left(\frac{2S_iB}{K}\right)^{-m} \tag{28}$$

Under constant amplitude loading failure occurs by definition when the total degree of damage $D_{tot} = \sum D_i$ attains the value D_{fail} equal to 1. However, with variable-amplitude random loading

the influences due to the load history may cause failure at the value D_{fail} different from 1. To take into account the uncertainty of the failure defintion, D_{fail} will be modelled as a random variable.

In fatigue analysis of jackets, the analysis will primarily focus on the welded joint between the members. When considering a fatigue failure in tubular joints the geometry of the whole nodal point becomes very important, since stress concentrations will occur due to the non-uniform stiffness of the chord wall and the brace. The locations, or points at which the highest stress occurs, are called hot spots. In welded joints two different hot spots for each brace in the joint are found, one at the weld toe on the brace side, the other on the chord side, i.e. for K-joints there are four hot spots. The stress concentration factor (SCF) is defined as the ratio of the hot spot stress σ_{max} to the nominal stress σ_N in the brace, i.e.

$$SCF = \frac{\sigma_{max}}{\sigma_N} \tag{29}$$

The SCF's for a given joint geometry and loads can be estimated either by full-scale tests or by a FEM-analysis. Here the SCF's are estimated by using some empirical formulas suggested by Kuang, [12], [13], which are based on thin shell FEM-analysis of different joint-geometry and loads. Two modes of fatigue failure, called failure elements, are defined to occur for each brace in a tubular joint, cracking at the hot spot toe of the weld jointing the brace to the chord (brace fatigue) and cracking at the hot spot in the wall of the chord itself (punching shear fatigue). The locations in the chord/brace intersection, where the hot spot stresses occur, depend on the external loads. In [12] it is recommended to check the 8 points along the brace/chord intersection to locate the hot spots, see figure 1.

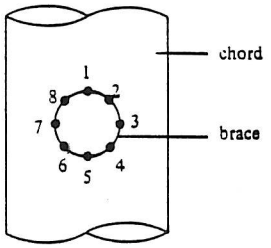

Figure 1. Points in the brace/chord intersection where the stress concentrations are checked.

For a given sea state, the mean fatigue damage of a failure element under consideration per stress amplitude, $\overline{D}_i$ can be determined by substituting eq.(26) and eq.(28) as:

$$\overline{D}_i = \int_0^\infty D_i(s)\; p_S(s) ds \tag{30}$$

where $p_S(s)$ is the distribution function of the stress amplitudes, see section 5.1.

The total damage in the failure element, D_{tot} is obtained by summing up the mean damage $\overline{D}_i$ over the service life of the structure, taking account of the long-term distribution of the sea states (see chapter 2):

$$D_{tot} = \int_{\overline{\theta}} \int_{H_s} \int_{T_p} \frac{T_L}{T_{mp}(t,h,\theta)} \overline{D}_i(t,h,\theta)\; p_{T_p|H_s}(t|h)\; p_{H_s}(h)\; p_{\overline{\theta}}(\theta)\; dt\, dh\, d\theta \tag{31}$$

where $p_{H_s}(h)$ is the marginal probability density function of the significant wave height H_s, $p_{T_p|H_s}(t|h)$ is the conditional probability density function of the wave spectral peak periods T_p, given H_s, $p_{\overline{\theta}}(\theta)$ is the probability density function of the mean direction of the wave propagation, $\overline{\theta}$, T_L is the total service life and T_{mp} is mean period of a stress cycle within the sea state.
The fatigue failure mode for the failure element is described by a safety margin M, defined as:

$$M = D_{fail} - D_{tot} \tag{32}$$

and the probability of failure P_f is

$$P_f = P(M \leq 0) \tag{33}$$

For a narrow-banded stress process $p_S(s)$ becomes Rayleigh distributed. $\overline{D}_i$ can be written as:

$$\overline{D}_i = \int_0^\infty B^m \left(\frac{2s}{K}\right)^m \frac{s}{\sigma_S^2} \, exp\left(-\frac{s^2}{2\sigma_S^2}\right) ds$$

$$= B^m \frac{\sigma_S^m}{K^m} \left(2\sqrt{2}\right)^m \Gamma(1+\frac{m}{2}) \tag{34}$$

where $\Gamma(\cdots)$ is the gamma function.

And the total degree of damage D_{tot} can be written as:

$$D_{tot} = \int_\theta \int_{H_s} \int_{T_p} \frac{T_L B^m}{T_{mp}(t,h,\theta)} \frac{\sigma_S^m(t,h,\theta)}{K^m} \left(2\sqrt{2}\right)^m \Gamma(1+\frac{m}{2})$$
$$p_{T_p|H_s}(t|h) \; p_{H_s}(h) \; p_{\overline{\theta}} \; dt \, dh \, d\theta \tag{35}$$

where T_{mp} can be estimated as:

$$T_{mp} = 2\,\pi \sqrt{\frac{m_0}{m_2}} \tag{36}$$

where m_0 and m_2 are the area and the second moment of the auto-spectral density of the stress spectra in the failure element.

In general, the safety margin M, as in eq.(32), is a function of the number of correlated non-normally distributed random variables $\overline{X} = (X_1, \ldots, X_n)$ called basic variables (where $\overline{X} = (D_{fail}, B, m, K)$), i.e. $M = f(\overline{X})$. $f(\overline{x})$ is called the failure function defined in such a way that it divides the n-dimensional basic variables space ω into two regions, namely a safe region ω_s, where $f(\overline{x}) > 0$, and an unsafe region ω_f, where $f(\overline{x}) \leq 0$. By a suitable transformation the correlated and non-normally distributed variables $\overline{X}$ are transformed into uncorrelated and standardized normally distributed variables $\overline{Z}$. By this transformation the failure surface is given by $f(\overline{z}) = 0$ in the corresponding z-space. In the n-dimensional z-space the reliability index β is defined as the shortest distance from the origin to the failure surface, i.e.

$$\beta = \min_{\overline{z} \in \partial\omega} \left(\sum_{i=1}^n z_i^2\right)^{\frac{1}{2}} \tag{37}$$

It can be shown that the probability of failure P_f in eq.(33) can be determined with good approximation from

$$P_f \approx \Phi(-\beta) \tag{38}$$

where $\Phi(\cdot)$ is the standard normal distribution function.

Until now a probability of failure for one failure element has been considered. When the probability of fatigue failure of the whole structure is considered the probabilities of failure for every failure element must be evaluated. If the largest of these probabilities of failure is used as a measure of the probability of fatigue failure of the structure this is called reliability modelling at level 0. A more satisfactory estimate of the probability of fatigue failure of the structure P_f^s is based on

systems approach (see [15]). This is called reliability modelling at level 1. The systems probability of fatigue failure can be estimated as:

$$P_f^s \approx 1 - \Phi_n(\overline{\beta}, \overline{\overline{\rho}}) \tag{39}$$

where n is the number of failure elements in the structure, Φ_n is the n-dimensional standardized normal distribution function, $\overline{\beta}$ $(= \beta_1, \ldots, \beta_n)$ the reliability indices for the failure elements and $\overline{\overline{\rho}}$ the correlation matrix for the safety margins. In real structures the number of failure elements n is very often very large, but usually a large number of failure elements is not significant for the systems reliability which means that evaluation of the systems probability of fatigue failure in eq.(39) becomes much less complicated.

6. APPLICATION

In the above chapters a method for estimating the probability of fatigue failure is briefly described. To make this method applicable a new computer package "SAOFF" (Stochastic Analysis Of Fatigue Failure) has been made. The program package which is written in FORTRAN, consists of five calculation blocks, namely:

1) STIFFMAS
This program reads the structural data and creates the global stiffness and mass matrices for the structure.

2) EIGEN
This program evaluates the n smallest eigenfrequencies and corresponding eigenvectors (mode shapes), where n is defined by the user.

3) MODAL
This program is the most complex and time-consuming part of the whole program package. Here the 0-,2- and 4-moments of the cross-spectral density of the modal displacements are evaluated, namely (see chapters 3 and 4 for more details):

0-moment:

$$\int_0^\infty S_{q_i q_j}(\omega) d\omega$$

2-moment:

$$\int_0^\infty \omega^2 S_{q_i q_j}(\omega) d\omega$$

4-moment:

$$\int_0^\infty \omega^4 S_{q_i q_j}(\omega) d\omega$$

4) SIGMA
In this program the auto-spectral densities and their moments for the hot spot stresses in joints defined by the user are evaluated. (Here the SCFs are taken into account in the calculation of T_{ki} and T_{kj}).

5) RELIA
In this program the probability of fatigue failure of failure elements in the joints (which was defined in SIGMA) is estimated. Here the user can choose between 3 different estimates of the distribution of the stress amplitudes $p_S(s)$, namely :
1) Rayleigh distribution (narrow-banded approach)

2) Distribution defined by the RFC-method (simulation)
3) Distribution defined by the RC-method (analytical estimation or simulation)
And the systems probability of fatigue failure is estimated by using Hohenbichler approximation (see chapter 5 for more details)

6.1 Example

Consider the model of a steel jacket offshore platform in figure 2. All structural elements are tubular beam elements made of steel with modulus of elasticity $E = 0.205 \cdot 10^9$ kN/m^2 and density $\rho = 7800$kg/m^3.
The cross-sectional diameters and thickness are shown in table 1. The foundation is modelled as elastic springs with horizontal stiffness equal to $1.2 \cdot 10^5$kN/m, vertical stiffness equal to 10^6 kN/m and rotational stiffness equal to $1.2 \cdot 10^6$kNm/rad. The total mass of the deck is assumed to be $4.8 \cdot 10^6$kg. The service life of the structure is taken as 25 years.
The calculation is carried out by considering 1 direction of wave propagation $\overline{\theta}$, namely $\overline{\theta}_1 = 0^o$ (x-direction), with the probability $p_{\overline{\theta}_1} = 1.0$ where $\overline{\theta}$ is defined in figure 2. Long crested waves are assumed ($n = 0$ in eq.(3)).

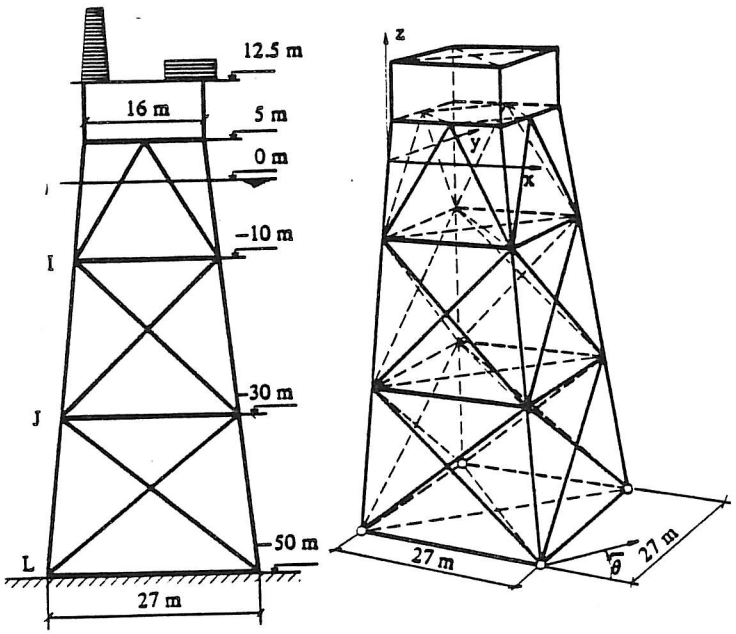

Figure 2. Steel jacket offshore platform.

The parameter in the long-term probability density function of the significant wave height H_s $p_{H_s}(h)$, and conditional probability density function of the wave spectral peak periods T_p give H_s, $p_{T_p|H_s}(t|h)$ are estimated by fitting observations from the northern part of the North Sea i the period 1980-1983 (8222 observations), see [19] for more details. The parameters are (see eq.(8 and eq.(9)):

$$\sigma^2_{H_s} = 0.376, \qquad \mu_{H_s} = 0.836, \qquad \upsilon = 3.27 \text{ m}, \qquad \rho = 2.822, \qquad \xi = 1.547$$

$$\mu_{T_p} = 1.59 + 0.42\ ln(h+2)$$

$$\sigma^2_{T_p} = 0.005 + 0.85\ exp\left(-0.13\ h^{1.35}\right)$$

Members	Diameter (m)	Thickness (m)
deck legs	2.00	0.050
jacket legs	1.20	0.016
braces (vertical plane)	1.20	0.016
braces (horizontal plane):		
level +5	0.80	0.008
level -10	1.20	0.014
level -30	1.20	0.014
level -30 (diagonal)	1.20	0.016
level -50	1.20	0.014

Table 1. Cross-sectional data for structural elements.

The total damage calculation for each failure element is carried out by considering 15 sea states, see table 2.

H_s (m)	p_{H_s}	T_p (sec)	$p_{T_p\|H_s}$
0.8	0.30924	5.8	0.366318
		7.9	0.442132
		11.5	0.191550
2.5	0.42741	7.1	0.306097
		9.2	0.447116
		12.6	0.246787
4.3	0.22634	8.9	0.331933
		10.6	0.439235
		14.0	0.228832
7.9	0.03621	11.2	0.293697
		12.8	0.432785
		14.9	0.273518
12.0	0.00080	13.6	0.312393
		14.9	0.452909
		16.7	0.234698

Table 2. The sea states under consideration and their probabilities.

In figure 2 two joints in the structure are considered, namely joints I and J (two TK-joints which give 12 failure elements). Detailed data and numbering of failure elements for the joints under consideration are shown in figure 3. The location of failure elements in the chord/brace intersection is determined by checking 8 points along the chord/brace intersection, see figure 1. The stochastic variables D_{fail} and B (see chapter 5.1) are assumed to be uncorrelated, but they are the assumed to be fully correlated between failure elements and with the same statistical characteristics, respectively. m and K are assumed to have correlation coefficient equal to -0.44 for each failure element, but uncorrelated between failure elements. The statistical characteristics for the stochastic variables are shown in table 3.

Basic variable	Variable	Distri-buted	Expected value	Standard deviation
X_1	D_{fail}	N	1.0	0.1
X_2	B	LN	1.0	0.2
$X_3, \ldots X_{18}$	$K_1, \ldots K_{16}$	LN	6400N/mm^2	1024N/mm^2
$X_{19}, \ldots X_{34}$	$m_1, \ldots m_{16}$	N	3.8	0.095

Table 3. Statistical characteristics for the stochastic variables (N: normal, LN: log-normal).

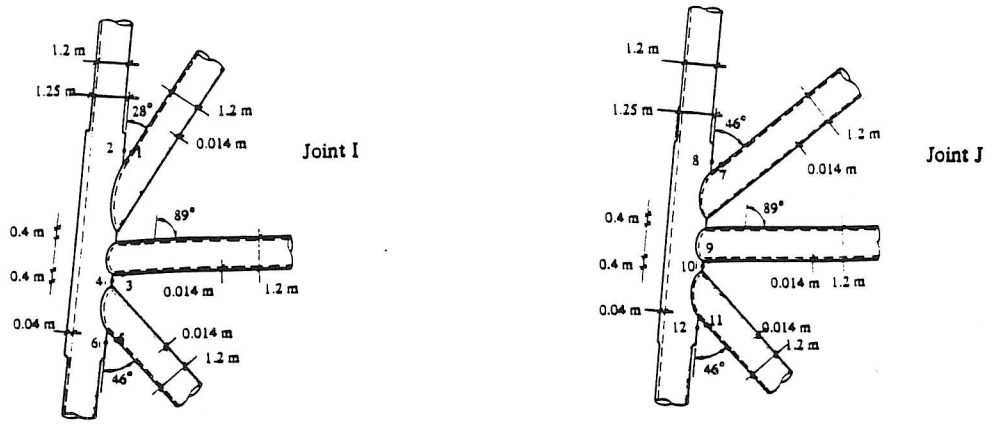

Figure 3. Detailed data and location of failure elements for joints under consideration (•·means failure element).

The drag coefficient C_D in Morison's equation is taken as 1.3, but the coefficient of inertia C_M is assumed to vary as [17]:

$$C_M = \begin{cases} 2 & \text{for } 0 \leq x \leq 0.6 \\ 2(1.65\ exp(-0.8974\ x)) & \text{for } 0.6 < x < 2.0 \\ 2(0.798/\sqrt{x^3}\ ) & \text{for } x \geq 2.0 \end{cases}$$

where $x = \frac{D}{2g}\ \omega^2$ in which D denotes a member diameter, g denotes the acceleration of gravity and ω is the frequency.

The number of eigenfrequencies (and mode shapes) in the modal analysis is taken as 3 and the damping ratio ζ is taken as 1 % for all mode shapes. The significant failure elements are defined as the failure elements which have safety indices less than $\beta_{min} + 2.1$, where β_{min} is the lowest safety index for the failure elements. The three lowest eigenfrequencies are obtained as:

$$\omega_1 = 3.01\ rad/sec$$
$$\omega_2 = 3.01\ rad/sec$$
$$\omega_3 = 6.48\ rad/sec$$

A run of the program SIGMA showed that the irregularity factor, α ($=\frac{m_2}{\sqrt{m_0\ m_4}}$, where m_i is the i^{th} moment of the stress spectra), of the stress spectra in the failure elements is 0.37-0.6 for most of the sea states which mean broad banded stress spectrum.
In figure 4 a typical normmalized stress spectrum (normalized as $m_0 = 1.0$) for the failure element ($H_s = 4.3$m, $T_p = 10.6$ sec, $\alpha = 0.51$).

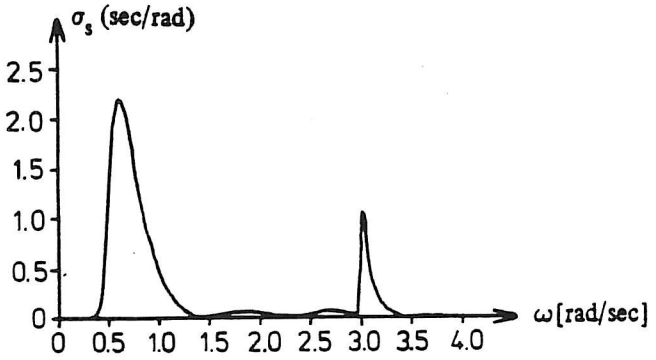

Figure 4. Typical normalized stress spectrum for the failure elements.

The distribution of stress amplitudes will be estimated by :

1 : Rayleigh distribution.

2 : Distribution defined by the RFC-method.

3 : Distribution defined by the RC-method.

Four not fully correlated significant failure elements are identified. They are given in table 4.

Failure element i	1	7	3	9	System reliability index β^s
Rayleigh β_i	1.70	1.71	3.46	3.80	1.45
RFC β_i	1.89	1.89	3.64	3.98	1.62
RC β_i	2.43	2.44	4.19	4.53	2.16

Table 4. Safety indices for the significant failure elements and Hohenbichler approximation of the system reliability index.

The correlation coefficient matrix of the linearized safety margins of the significant failure elements is:

$$\bar{\bar{\rho}} = \begin{bmatrix} 1.0 & 0.65 & 0.65 & 0.65 \\ & 1.0 & 0.65 & 0.65 \\ \text{sym.} & & 1.0 & 0.65 \\ & & & 1.0 \end{bmatrix}$$

As we can see from table 4, there are significant differences between the safety indices of a failure element dependent on how the distribution of the stress amplitudes is estimated and it is especially interesting to see the significant difference between the probability density functions estimated by the RFC and the RC methods, see figure 5.

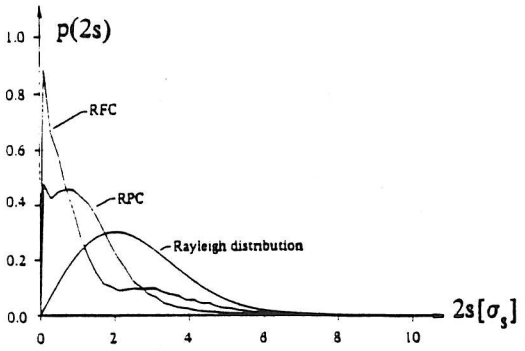

Figure 5. Estimation of the distribution density function of the stress amplitude based on simulation and using RFC- and the RC-methods.

7. CONCLUSIONS

- A method to estimate the reliability of offshore structures subjected to wave loads in deep water environments is presented.
- Failure modes corresponding to fatigue failure are used.
- The reliability is estimated using a first-order reliability method.
- The statistically measured of structural stress variations is estimated by using modal spectral analysis method.

- The damage in the failure elements is estimated by using Miner's rule and S-N approach.
- The distribution function of the stress amplitudes, for a given sea state, is estimated by Rayleigh distribution, Rice distribution, RFC-method and RC-method.
- For most of the sea states under consideration the stress process became broad-banded and therefore, the results by using Rayleigh distribution cannot be expected to give satisfactory results.
- The RFC and RC methods give a different estimation of the distribution function of the stress amplitudes, resulting in a major difference in the estimate of the safety indices.
- This means that the order and definition of the stress amplitudes must be taken into account in the damage accumulation model.
- For this purpose more experimental and theoretical work are needed.

REFERENCES

[1] Watt, B. J.: *Basic Structural System - A Review of Their Design and Analysis Requirements.* Numerical Methods in Offshore Engineering, 1978.

[2] Sigbjørnsson, R.: *Stochastic Theory of Wave Loading Processes.* Eng. Struct., Vol. 1, January 1979, pp.58-64.

[3] Sigbjørnsson, R. & E. K. Smith: *Wave Induced Vibrations of Gravity Platforms: A Stochastic Theory.* Applied Mathematical Modelling, Vol. 4, June 1980, pp.155-165.

[4] Sarpkaya, T. & M. Isaacson: *Mechanics of Wave Forces on Offshore Structures.* van Nostrand Reinhold Co., 1981.

[5] Haver, S.: *Long-Term Response Analysis - Advantages and Present Limitations.* Paper presented at the "Deep Water Jacket Seminar", Statoil, Trondheim, August 1985.

[6] Sigbjørnsson, R., K. Bell & I. Holand: *Dynamic Response of Framed and Gravity Structures to Waves.* Numerical Methods in Offshore Engineering, 1978.

[7] Olufsen, A., K. A. Farnes & D. Fergestad: *FAROW - A Computer Program for Dynamic Response Analysis and Fatigue Life Estimation of Offshore Structures Exposed to Ocean Waves - Theoretical Manual.* SINTEF, Report STF71 A86040, ISBN No:82-595-4318-4. 1986.

[8] Haver, S.: *Wave Climate of Northern Norway.* Applied Ocean Research, Vol. 7, No. 2 1985, pp.85-92

[9] Atalik, T. S. & S. Utku: *Stochastic Linearization of Multi-Degree-of-Freedom Non-Linear System.* Earthquake Engiveering and Structural Dynamics, Vol. 4, 1976, pp. 411-420.

[10] Langen, I. & R. Sigbjørnsson: *Dynamisk Analyse av Konstruksjoner* (in Norwegian) Tapir Publishers, Trondheim, 1979.

[11] Cronin, D. J., P. S. Godfrey, P. M. Hook & T. A. Wyatt: *Spectral Fatigue Analysis for Offshore Structures.* Numerical Methods in Offshore Engineering, 1978.

[12] Almar-Næs, A.(ed).: *Fatigue Handbook.* Tapir Publishers, Trondheim, 1985.

[13] Dansk Standard DS 449. *Danish Code of Practice for Pile-Supported Offshore Steel Structures.* Teknisk Forlag, april 1983. ISBN 87-571-0838-2.

[14] Baker, M. J.: *Supplementary Notes on Fatigue and Fracture Reliability of Offshore Structures.* Structural Safety and Reliability: Theory and Practice, Short Course, September 1985.

[15] Thoft-Christensen, P. & Y. Murotsu: *Application of Structural Systems Reliability Theory.* Springer-Verlag, 1986.

[16] Lin, Y. K.: *Probabilistic Theory of Structural Dynamices.* McGraw-Hill, 1967.

[17] Karadeniz, H.: *Stochastic Analysis Program for Offshore Structures (SAPOS).* Report, Department of Civil Engineering, Delft University of Technology, Delft, Netherlands, May 1985.

[18] Hohenbichler, M.: *An Approximation to the Multivariate Normal Distribution.* DIALOG 6-82, Danish Academy of Engineers, Lyngby, 1982, pp.79-100.

[19] Haver, S. & K. A. Nyhus.: *Wave Climate Elevation for Design Purposes.* 5th OMAE, Tokyo, April 1986.

[20] Wirsching P. H. & A. M. Shehata.: *Fatigue Under Wide Band Stresses Using the Rain-Flow Method.* Journal of Engineering Materials and Technology, July 1977, pp.205-211.

APPENDIX A

This appendix deals with three-dimensional linearization of drag forces by the "minimum mean square error linearization method" [9]. A circular cylinder as shown in figure A1 is considered, and it is assumed that Morison's equation may be applied to a cylindrical member in a random manner. The non-linear term in Morison's equation may be written as:

$$\overline{f}_D = \begin{bmatrix} f_{Dx} \\ f_{Dy} \\ f_{Dz} \end{bmatrix} = K_D \, |\overline{\dot{u}}_n| \, \overline{\dot{u}}_n = K_D \, (\dot{u}_{nx}^2 + \dot{u}_{ny}^2 + \dot{u}_{nz}^2)^{\frac{1}{2}} \begin{bmatrix} \dot{u}_{nx} \\ \dot{u}_{ny} \\ \dot{u}_{nz} \end{bmatrix} \tag{A1}$$

where

$$\overline{\dot{u}}_n = \begin{bmatrix} \dot{u}_{nx} \\ \dot{u}_{ny} \\ \dot{u}_{nz} \end{bmatrix} = \overline{c}(\overline{\dot{u}}^T \times \overline{c}) = \begin{bmatrix} 1-c_x^2 & -c_x c_y & -c_x c_z \\ & 1-c_y^2 & -c_y c_z \\ \text{sym.} & & 1-c_z^2 \end{bmatrix} \begin{bmatrix} \dot{u}_x \\ \dot{u}_y \\ \dot{u}_z \end{bmatrix} \tag{A2}$$

$\overline{c} \;\; = (c_x, c_y, c_z)$

$\overline{\dot{u}}^T = (\dot{u}_x, \dot{u}_y, \dot{u}_z)$

$\dot{u}_x$, $\dot{u}_y$ and $\dot{u}_z$ are components of the water particle velocity in the x, y and z-direction, respectively, and $\overline{c}$ is a unit vector along the cylinder axis.

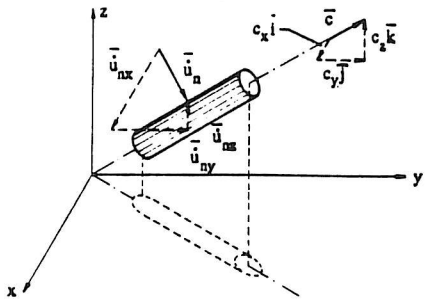

Figure A1. $\overline{i}$, $\overline{j}$ and $\overline{k}$ represent the base vectors in the x, y, z-coordinate system.

The linearized version of equation (A1) is

$$\overline{f}_{DL} = K_D \, \overline{\overline{L}} \, \overline{\dot{u}}_n \tag{A3}$$

where $\overline{\overline{L}}$ is the linearization coefficient matrix, expressed as:

$$\overline{\overline{L}} = \begin{bmatrix} l_{xx} & l_{xy} & l_{xz} \\ l_{yx} & l_{yy} & l_{yz} \\ l_{zx} & l_{zy} & l_{zz} \end{bmatrix}$$

The error introduced by using equation (A3) instead of equation (A1) is defined as:

$$\bar{e} = (\bar{\bar{L}}\,\bar{\dot{u}}_n \;-\; \bar{g}(\bar{\dot{u}}_n)\;) \tag{A4}$$

where

$$\bar{g}(\bar{\dot{u}}_n) = \begin{bmatrix} g_x(\bar{\dot{u}}_n) \\ g_y(\bar{\dot{u}}_n) \\ g_z(\bar{\dot{u}}_n) \end{bmatrix} = (\dot{u}_{nx}^2 + \dot{u}_{ny}^2 + \dot{u}_{nz}^2)^{\frac{1}{2}} \begin{bmatrix} \dot{u}_{nx} \\ \dot{u}_{ny} \\ \dot{u}_{nz} \end{bmatrix}$$

The criterion that the mean square value of the error $\bar{e}$ is at a minimum is expressed as:

$$E[\bar{e}\;\bar{e}^T]. \rightarrow \text{minimum}$$

where $E[\cdots]$ denotes the expected value.

The coefficients l_{ij} in the linearization matrix $\bar{\bar{L}}$ may be written as [9],[10]:

$$l_{ij} = E[\;\frac{\partial g_i(\bar{\dot{u}}_n)}{\partial \dot{u}_{nj}}] \tag{A5}$$

The matrix $\bar{\bar{L}}$ may now be expressed as:

$$\bar{\bar{L}} = E\begin{bmatrix} \frac{2\dot{u}_{nx}^2+\dot{u}_{ny}^2+\dot{u}_{nz}^2}{|\bar{\dot{u}}_n|} & \frac{\dot{u}_{nx}\dot{u}_{ny}}{|\bar{\dot{u}}_n|} & \frac{\dot{u}_{nx}\dot{u}_{nz}}{|\bar{\dot{u}}_n|} \\ & \frac{\dot{u}_{nx}^2+2\dot{u}_{ny}^2+\dot{u}_{nz}^2}{|\bar{\dot{u}}_n|} & \frac{\dot{u}_{ny}\dot{u}_{nz}}{|\bar{\dot{u}}_n|} \\ \text{sym.} & & \frac{\dot{u}_{nx}^2+2\dot{u}_{ny}^2+\dot{u}_{nz}^2}{|\bar{\dot{u}}_n|} \end{bmatrix} = E[\bar{\bar{M}}]$$

where $|\bar{\dot{u}}_n| = (\dot{u}_{nx}^2 + \dot{u}_{ny}^2 + \dot{u}_{nz}^2)^{\frac{1}{2}}$.

When the water particle velocity is assumed to be a zero-mean Gaussian process then the following expression is obtained

$$E[\bar{\bar{M}}] = \int_{-\infty}^{\infty}\int_{-\infty}^{\infty}\int_{-\infty}^{\infty} \bar{\bar{M}} N_3(0, \bar{\bar{\Sigma}}_{\dot{u}_x\dot{u}_y\dot{u}_z}) d\dot{u}_x d\dot{u}_y d\dot{u}_z \tag{A6}$$

where $N_3(0, \bar{\bar{\Sigma}}_{\dot{u}_x\dot{u}_y\dot{u}_z})$ is a three-dimensional normal density function defined by:

$$N_3(0, \bar{\bar{\Sigma}}_{\dot{u}_x\dot{u}_y\dot{u}_z}) = \frac{1}{(2\pi)^{3/2}(det(\bar{\bar{\Sigma}}_{\dot{u}_x\dot{u}_y\dot{u}_z}))^{1/2}} exp(-\frac{1}{2}\bar{\dot{u}}^T \bar{\bar{\Sigma}}^{-1}_{\dot{u}_x\dot{u}_y\dot{u}_z}\;\bar{\dot{u}})$$

where the covariance matrix $\bar{\bar{\Sigma}}_{\dot{u}_x\dot{u}_y\dot{u}_z}$ is defined by:

$$\bar{\bar{\Sigma}}_{\dot{u}_x\dot{u}_y\dot{u}_z} = \begin{bmatrix} \int_0^\infty S_{\dot{u}_x\dot{u}_x}(\omega)d\omega & \int_0^\infty S_{\dot{u}_x\dot{u}_y}(\omega)d\omega & \int_0^\infty S_{\dot{u}_x\dot{u}_z}(\omega)d\omega \\ \int_0^\infty S_{\dot{u}_y\dot{u}_x}(\omega)d\omega & \int_0^\infty S_{\dot{u}_y\dot{u}_y}(\omega)d\omega & \int_0^\infty S_{\dot{u}_y\dot{u}_z}(\omega)d\omega \\ \int_0^\infty S_{\dot{u}_z\dot{u}_x}(\omega)d\omega & \int_0^\infty S_{\dot{u}_z\dot{u}_y}(\omega)d\omega & \int_0^\infty S_{\dot{u}_z\dot{u}_z}(\omega)d\omega \end{bmatrix}$$

$S_{\dot{u}_i \dot{u}_j}(\omega)$ is the cross-spectral density of the water particle velocity $\dot{u}_i$ and $\dot{u}_j$ $(i, j = x, y, z)$. Thus,

$$l_{xx} = E[m_{11}] = \int_{-\infty}^{\infty}\int_{-\infty}^{\infty}\int_{-\infty}^{\infty} \frac{2\dot{u}_{nx}^2 + \dot{u}_{ny}^2 + \dot{u}_{nz}^2}{|\bar{\dot{u}}_n|} \frac{1}{(2\pi)^{3/2}(det(\bar{\bar{\Sigma}}_{\dot{u}_x \dot{u}_y \dot{u}_z}))^{1/2}}$$

$$exp(-\frac{1}{2}\bar{\dot{u}}^T \bar{\bar{\Sigma}}^{-1}_{\dot{u}_x \dot{u}_y \dot{u}_z} \bar{\dot{u}}) d\dot{u}_x d\dot{u}_y d\dot{u}_z$$

where $\dot{u}_{nx}$, $\dot{u}_{ny}$ and $\dot{u}_{nz}$ can be expressed as functions of $\dot{u}_x$, $\dot{u}_y$ and $\dot{u}_z$ (see eq. (A2)).

STRUCTURAL RELIABILITY THEORY SERIES

PAPER NO. 21: S. R. K. Nielsen & J. D. Sørensen: *Approximation to the Probability of Failure in Random Vibration by Integral Equation Methods.* ISSN 0105-7421 R8618.

PAPER NO. 22: P. Thoft-Christensen & J. D. Sørensen: *Optimal Strategy for Inspection and Repair of Structural Systems.* ISSN 0105-7421 R8619.

PAPER NO. 23: P. Thoft-Christensen & J. D. Sørensen: *Reliability Analysis of Tubular Joints in Offshore Structures.* ISSN 0105-7421 R8620.

PAPER NO. 24: G. Sigurdsson: *Development of Applicable Methods for Evaluating the Safety of Offshore Structures, Part 4.* ISSN 0105-7421 R8701.

PAPER NO. 25: M. H. Faber & P. Thoft-Christensen: *Instability and Buckling Failure Elements for Columns.* ISSN 0105-7421 R8702.

PAPER NO. 26: P. Thoft-Christensen & M. H. Faber: *Deflection and Global Instability Failure Elements for Geometrical Non-Linear Structures.* ISSN 0902-7513 R8706.

PAPER NO. 27: K. J. Mørk, P. Thoft-Christensen & S. R. K. Nielsen: *Simulation Studies of Joint Response Statistics for a One-Degree-of-Freedom Structure.* ISSN 0902-7513 R8707.

PAPER NO. 28: P. Thoft-Christensen, S. R. K. Nielsen & K. J. Mørk: *Simulation Studies of Joint Response Statistics for Two-Storey Hysteretic Frame Structures.* ISSN 0902-7513 R8708.

PAPER NO. 29: J. D. Sørensen & P. Thoft-Christensen: *Integrated Reliability -Based Optimal Design of Structures.* ISSN 0902-7513 R8709.

PAPER NO. 30: S. R. K. Nielsen, K. J. Mørk & P. Thoft-Christensen: *Reliability Analysis of Hysteretic Multi-Storey Frames under Random Excitation.* ISSN 0902-7513 R8711.

PAPER NO. 31: J. D. Sørensen & Rune Brincker: *Simulation of Stochastic Loads for Fatigue Experiments.* ISSN 0902-7513 R8717.

PAPER NO. 32: J. D. Sørensen: *Reliability-Based Optimization of Structural Systems.* ISSN 0902-7513 R8718.

PAPER NO. 33: P. Thoft-Christensen: *Application of Optimization Methods in Structural Systems Reliability Theory.* ISSN 0902-7513 R8719.

PAPER NO. 34: P. Thoft-Christensen: *Recent Advances in the Application of Structural Systems Reliability Methods.* ISSN 0902-7513 R8721.

PAPER NO. 35: P. Thoft-Christensen: *Applications of Structural Systems Reliability Theory in Offshore Engineering. State-of-the-Art.* ISSN 0902-7513 R8722.

PAPER NO. 36: J. D. Sørensen: *PRADSS: Program for Reliability Analysis and Design of Structural Systems.* First Draft. ISSN 0902-7513 R8724.

STRUCTURAL RELIABILITY THEORY SERIES

PAPER NO. 37: Jan Kazimierz Szmidt: *Discrete Analysis of a Plane Initial-Value Problem for an Offshore Structure.* ISSN 0902-7513 R8801.

PAPER NO. 38: M. H. Faber & P. Thoft-Christensen: *Modelling of Floor Loads.* ISSN 0902-7513 R8802.

PAPER NO. 39: S. R. K. Nielsen, K. J. Mørk & P. Thoft-Christensen: *Stochastic Response of Hysteretic Systems.* ISSN 0902-7513 R8803.

PAPER NO. 40: P. Thoft-Christensen & G. B. Pirzada: *Upper-Bound Estimate of the Reliability of Plastic Slabs.* ISSN 0902-7513 R8804.

PAPER NO. 41: S. R. K. Nielsen, K. J. Mørk & P. Thoft-Christensen: *Response Analysis of Hysteretic Multi-Storey Frames under Earthquake Excitation.* ISSN 0902-7513 R8805.

PAPER NO. 42: J. D. Sørensen: *Probabilistic Design of Offshore Structural Systems.* ISSN 0902-7513 R8806.

PAPER NO. 43: S. G. Zhang & P. Thoft-Christensen: *Tool Life Reliability.* ISSN 0902-7513 R8807.

PAPER NO. 44: K. J. Mørk, S. R. K. Nielsen & P. Thoft-Christensen: *Probability Distributions of Damage Indicators in Hysteretic Structures.* ISSN 0902-7513 R8817.

PAPER NO. 45: J. D. Sørensen: *Optimal Design with Reliability Constraints.* ISSN 0902-7513 R8818.

PAPER NO. 46: S. G. Zhang & P. Thoft-Christensen: *Experimental Testing and Monitoring of Tool Wear.* ISSN 0902-7513 R8819.

PAPER NO. 47: P. Thoft-Christensen: *Consequence Modified β-Unzipping of Plastic Structures.* ISSN 0902-7513 R8820.

PAPER NO. 48: J. D. Sørensen & P. Thoft-Chrisstensen: *Inspection Strategies for Concrete Bridges.* ISSN 0902-7512 R8825.

PAPER NO. 49: M. Delmar, J. D. Sørensen & P. Thoft-Christensen: *Collapse Probability of Elasto-Plastic Structures.* ISSN 0902-7513 R8827.

PAPER NO. 50: G. Sigurdsson: *Stochastic Fatigue Analysis of Jacket Type Offshore Structures.* ISSN 0902-7513 R8828.

PAPER NO. 51: S. R. K. Nielsen: *Approximations to the Probability of Failure in Random Vibration by Integral Equation Methods.* ISSN 0902-7513 R8829.

INSTITUTE OF BUILDING TECHNOLOGY AND STRUCTURAL ENGINEERING
THE UNIVERSITY OF AALBORG
SOHNGAARDSHOLMSVEJ 57. DK 9000 AALBORG
TELEPHONE: Int. + 45 – 8 – 14 23 33